



Comparative kinetic studies on tyrosinase-like catalytic activity of dinuclear imidazole-containing copper(II) complexes

Wendel Andrade Alves^a, Saulo Afonso de Almeida-Filho^a,
Mauro Vieira de Almeida^b, Armando Paduan-Filho^c,
Carlos Castilla Becerra^c, Ana Maria Da Costa Ferreira^{a,*}

^a Departamento de Química Fundamental, Instituto de Química, Universidade de São Paulo,
P.O. Box 26077, São Paulo 05513-970, SP, Brazil

^b Universidade Federal de Juiz de Fora, Juiz de Fora, MG, Brazil

^c Instituto de Física, Universidade de São Paulo, São Paulo, SP, Brazil

Received 26 September 2002; received in revised form 4 December 2002; accepted 2 January 2003

Abstract

Comparative kinetic studies on the catalytic activity of some new dinuclear copper(II) complexes in the oxidation of phenolic and catechol substrates are reported. These complexes, showing a tri- or tetradentate imine ligand containing an imidazole group, or additionally an imidazolate- or phenolate bridge between the copper ions, were synthesized and characterized by UV-Vis, IR, and EPR spectroscopy, and molar conductivity. Magnetic susceptibility measurements in the solid state, in the temperature range 2–300 K, indicated an anti-ferromagnetic coupling of the copper(II) centers for all the species studied. These compounds exhibited in aqueous solution an equilibrium between the dinuclear and the corresponding mononuclear species, very dependent of the pH. Their catalytic activity in the oxidation of 2,6-di-*tert*-butylphenol, and of 3,4-dihydroxyphenylalanine (L-dopa) was monitored in methanol solution, following the corresponding quinone formation, at 418 nm ($\epsilon = 5.48 \times 10^4 \text{ mol}^{-1} \text{ l cm}^{-1}$), or at 475 nm ($\epsilon = 3.60 \times 10^3 \text{ mol}^{-1} \text{ l cm}^{-1}$), respectively. Differing in some structural features, their tyrosinase-like catalytic activity was verified to be influenced by several factors, including hydrophobic character, and steric hindrance of the ligands, accessibility of the oxidant to the catalytic center, and mainly by the stability of the dinuclear species in solution.

© 2003 Elsevier Science B.V. All rights reserved.

Keywords: Copper(II) complexes; Dinuclear species; Bioinorganic chemistry; Catalysis; Oxidation

1. Introduction

Copper protein mimics have been of huge interest for many years, especially those that simulate the structural or functional properties of enzymes associated to the molecular oxygen reactivity [1]. The

catalyzed oxidation of phenols, and amines is performed, *in vivo*, at very inspiring active sites, where the two-electron transfer occurs between the substrate and two metal centers, as in tyrosinase and catechol oxidase [2], or one metal center and a radical forming co-factor, as in amine oxidase [3]. Many of the reported studies are focused on the simulation of the structural, and spectral properties of those centers [4], as well as on O₂-activation mechanisms [5]. However, further interest in this type of reactivity is stimulated

* Corresponding author. Tel.: +55-11-3091-2151;
fax: +55-11-3815-5579.
E-mail address: amdcferr@iq.usp.br (A.M.D.C. Ferreira).

by industrial application of possible catalysts for obtaining essential products [6], elucidation of undesirable enzymatic browning of fruits [7], or application in medical diagnosis for the determination of brain catecholamines in severe neurological disorders [8].

Tyrosinases are found in a wide variety of plants, fungi, bacteria, mammals and insects, and catalyze the hydroxylation of tyrosine to dopa (cresolase activity), and the subsequent oxidation of dopa to dopaquinone (catecholase activity), with efficient electron transfer to dioxygen. In mammals, tyrosinases initiate the formation of melanin, responsible for pigmentation. Catechol oxidases, on the other hand, can be obtained from plants and fruits, and exclusively catalyze the oxidation of catechol to the corresponding quinone [9]. Both proteins have been extensively investigated in the last years, showing a characteristic type 3-copper center, with two copper atoms anti-ferromagnetically coupled ($-2J > 600 \text{ cm}^{-1}$), in the *met* form, Cu(II)–Cu(II). EXAFS measurements on catechol oxidase from sweet potatoes (*Ipomoea batatas*) indicated a Cu–Cu distance of 2.9 Å for the *met* state, and 3.8 Å in the *oxy* state. Similar XANES and EXAFS spectra revealed a 3.6 Å distance for the *oxy*-tyrosinase from *Neurospora crassa* [9a]. However, interesting features of the structure and activity of these enzymes were uncovered by additional bioinorganic studies involving mimics. In these studies, a large number of binuclear compounds were prepared and characterized by many workers, with different bridge groups or dinucleating ligands [10–12].

We have previously reported an imidazole-bridged copper(II) complex with tridentate ligands that efficiently catalyzed the aerobic oxidation of 2,6-di-*tert*-butylphenol, in methanolic solution, and also of 3,4-dihydroxyphenylalanine (L-dopa) in aqueous solution, in the range of pH 7–11 [13]. This complex coexist in aqueous solution with the corresponding mono- and tetranuclear species, depending on the pH. Herein we report the synthesis, and structural characterization of some new dinuclear imine–copper(II) complexes (shown in Fig. 1), subsequently investigated as models of the tyrosinase and catechol oxidase enzymes, and compared with previously related complexes.

In this work, we are particularly interested in a better understanding of those factors that can lead to more effective catalysis by copper(II) ions in reactions with molecular dioxygen. Systematic studies that se-

lectively change the structural and electronic features of copper complexes, and assess the corresponding effect on their catalytic properties could help to explain which features are primarily responsible for its activity. In addition, studies of this type would assist rational design and synthesis of more efficient catalysts [14].

2. Experimental

All reagents were of analytical grade, purchased from different sources, and used without further purification. The following abbreviations were used:

apip	2-[2-(2-pyridyl)ethylimino-1-ethyl]pyridine, ligand derived from 2(2-aminoethyl)pyridine and 2-acetylpyridine;
apbz	2-[3-(1-benzylamino)propylimino-1-ethyl]pyridine, ligand derived from <i>N</i> -benzyl-1,3-propanediamine and 2-acetylpyridine;
apph	2-[2-(phenylamine)imino-1-ethyl]pyridine, ligand derived from 1,2-phenylenediamine and 2-acetylpyridine;
2-iensal	ligand derived from 2-imidazolecarboxaldehyde, ethylenediamine, and salicylaldehyde;
imH	imidazole; im, imidazolate anion;
2-iphals	ligand derived from 2-imidazolecarboxaldehyde, 1,2-phenylenediamine, and salicylaldehyde;
SE	2-salicylidene-aminoethane, ligand derived from salicylaldehyde and 1,2-diaminoethane.

2.1. Preparation of *N*-benzyl-1,3-propanediamine

N-Benzyl-1,3-propanediamine, used in the synthesis of the ligand apbz, was prepared by very slow addition of benzyl chloride (1.27 g; 10 mmol) to a solution of 1,3-propanediamine (2.96 g, or 40 mmol, dissolved in 20 ml of ethanol), during 8 h. After stirring the solution at room temperature for more 48 h, a saturated solution of NaOH in methanol was added, adjusting the final pH to 14. The solvent was then evaporated, and the residue purified by column chromatography, using a mixture of dichloromethane and methanol as

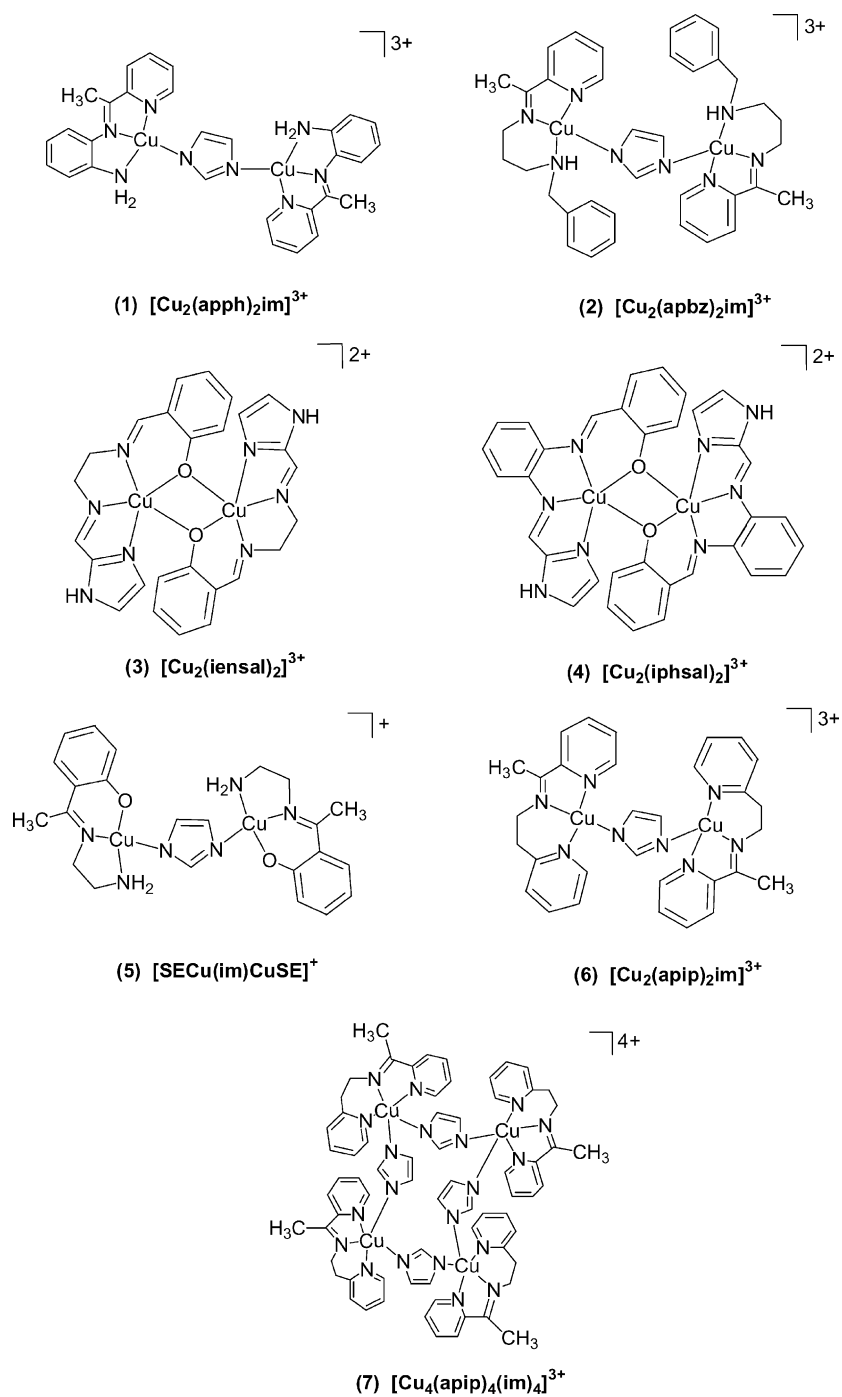


Fig. 1. Schematic structure of the copper(II) complexes studied.

eluent. Yield: 1.15 g (70%). mp: 305.5–307.5 °C. ^1H NMR (200 MHz; $\text{CF}_3\text{CO}_2\text{D}$) δ : 2.12 (m, 2H, CH_2); 3.09 (m, 4H, CH_2N); 4.06 (s, 2H, CH_2Ph); 7.15 (m, 5H, Ph). ^{13}C NMR (50 MHz, $\text{CF}_3\text{CO}_2\text{D}$) δ : 26.17; 40.25; 47.06; 55.60 (CH_2); 108.50; 114.14; 120.77; 125.41 (Ph).

2.2. Syntheses of the copper(II) complexes

Caution: Although the prepared species were shown to be very stable, perchlorate salts of metal complexes with organic ligands are potentially explosive, and should be very carefully handled, only in small amounts.

All the copper complexes were prepared in methanol solutions, in small amounts (1–2 mmol), according to previously described procedure [13]. The compounds $[\text{SECuimCuSE}]$, $[\text{Cu}(\text{apip})\text{imH}](\text{ClO}_4)_2$, $[\text{Cu}_2(\text{apip})_2\text{im}](\text{ClO}_4)_3 \cdot \text{H}_2\text{O}$ and the tetranuclear species, $[\text{Cu}_4(\text{apip})_4(\text{im})_4](\text{ClO}_4)_4 \cdot 2\text{H}_2\text{O}$, have been previously obtained and characterized, as described elsewhere [13].

2.2.1. $[\text{Cu}_2(\text{apph})_2\text{im}](\text{ClO}_4)_3$ (**1**) and $[\text{Cu}_2(\text{apbz})_2\text{im}](\text{ClO}_4)_3$ (**2**)

New dinuclear complexes with diimine ligands, derived from 2-acetylpyridine and 1,2-phenylenediamine, or *N*-benzyl-1,3-propanediamine, $[\text{Cu}_2(\text{apph})_2\text{im}](\text{ClO}_4)_3$ (**1**), and $[\text{Cu}_2(\text{apbz})_2\text{im}](\text{ClO}_4)_3$ (**2**), respectively, were isolated by very similar procedures, with yields around 90%. Anal. compound (**1**), Calc, for $\text{C}_{29}\text{H}_{29}\text{N}_8\text{Cu}_2(\text{ClO}_4)_3$: C, 38.06; H, 3.19; N, 12.24. Found: C, 38.25; H, 3.78; N, 11.81. $A_M = 198.1 \text{ S cm}^2 \text{ mol}^{-1}$ in DMF. IR: $\nu(\text{OH})$, 3429; $\nu(\text{N-H})$, 3250, $\nu(\text{C=N})$, 1625; 3250; $\nu(\text{Cl-O})$, 1088, 631. Anal. compound (**2**), Calc, for $\text{C}_{37}\text{H}_{43}\text{N}_8\text{Cu}_2(\text{ClO}_4)_3$: C, 43.26; H, 4.22; N, 10.93. Found: C, 44.03; H, 4.16; N, 11.23. $A_M = 172.0 \text{ S cm}^2 \text{ mol}^{-1}$ in DMF. IR: $\nu(\text{OH})$, 3440; $\nu(\text{N-H})$, 3135; $\nu(\text{C=N})$, 1625; $\nu(\text{Cl-O})$, 1091, 626.

2.2.2. $[\text{Cu}_2(\text{iensal})_2](\text{ClO}_4)_2$ (**3**) and $[\text{Cu}_2(\text{iphsal})_2](\text{ClO}_4)_2 \cdot \text{CH}_3\text{OH}$ (**4**)

Ethylenediamine (70 μl , 1 mmol), or 1,2-phenylenediamine (108 mg, 1 mmol), in methanol (10 ml), was added dropwise to a solution of 2-imidazolecarboxaldehyde (99 mg, 1 mmol) in methanol (10 cm^3), and the mixture was stirred at 50 °C, for 1 h. During

this time the solution turned yellow. A solution of $\text{Cu}(\text{ClO}_4)_2 \cdot 6\text{H}_2\text{O}$ (378 mg, 1 mmol) in methanol (5 ml) was then added at once, under stirring, at room temperature. After 1 h, a solution of salicylaldehyde (0.11 ml, 1 mmol) in 5 ml methanol was slowly added. A greenish-yellow color was observed for the solution containing ethylenediamine as one of the reagents, or dark-yellow for the solution containing 1,2-phenylenediamine. The final solution was reduced to half of the volume, after being kept in freezer for 3 days. The crystals obtained were filtered off, washed with cooled diethyl ether, in the case of compound $[\text{Cu}_2(\text{iensal})_2](\text{ClO}_4)_2$ **3** (red color), or with cooled methanol and diethyl ether, for the compound $[\text{Cu}_2(\text{iphsal})_2](\text{ClO}_4)_2 \cdot \text{CH}_3\text{OH}$ **4** (dark-yellow color), and finally dried in vacuum. The compound **4** was recrystallized using methanol as solvent. The obtained yield was 53% for $[\text{Cu}_2(\text{iensal})_2](\text{ClO}_4)_2$, and 22% for $[\text{Cu}_2(\text{iphsal})_2](\text{ClO}_4)_2 \cdot \text{CH}_3\text{OH}$. Anal. compound **3**, Calc, for $\text{C}_{26}\text{H}_{26}\text{N}_8\text{O}_2\text{Cu}_2(\text{ClO}_4)_2$: C, 38.60; H, 3.24; N, 13.86. Found: C, 38.82; H, 3.25; N, 13.90. $A_M = 182.0 \text{ S cm}^2 \text{ mol}^{-1}$ in water, and $200 \text{ S cm}^2 \text{ mol}^{-1}$ in methanol. IR: $\nu(\text{O-H})$, 3449; $\nu(\text{N-H})$, 3200, 3156; $\nu(\text{C=N})$, 1630; $\nu(\text{Cl-O})$, 1109, 628. Anal. compound **4**, Calc, for $\text{C}_{34}\text{H}_{26}\text{N}_8\text{O}_2\text{Cu}_2(\text{ClO}_4)_2 \cdot \text{CH}_3\text{OH}$: C, 44.61; H, 3.53; N, 11.57. Found: C, 45.35; H, 3.42; N, 11.01. $A_M = 118.0 \text{ S cm}^2 \text{ mol}^{-1}$ in methanol. IR: $\nu(\text{O-H})$, 3521; $\nu(\text{N-H})$, 3183, 3137; $\nu(\text{C=N})$, 1609; $\nu(\text{Cl-O})$, 1107, 625.

2.3. Physical measurements

Elemental analyses were performed at the Central Analítica of our Institution, using a Perkin-Elmer 2400 CHN Elemental Analyser. Electronic spectra were registered in a Beckman DU-70 spectrophotometer, or an Olis modernized-Aminco DW 2000 instrument, with thermostated cell compartment. EPR spectra were recorded in a Bruker EMX instrument, operating at X-band frequency, using standard Wilmad quartz tubes, at 77 K. DPPH (α, α' -diphenyl- β -picrylhydrazyl) was used as frequency calibrant ($g = 2.0036$) for powder samples, and $[\text{Cu}(\text{edta})]^{2+}$ solutions (1.00 mmol dm^{-3}) as standard for frozen solutions. Infrared spectra of the complexes obtained were recorded in a BOMEM 3.0 instrument, in the range 4000–400 cm^{-1} , using KBr pellets. The temperature dependence of the magnetic susceptibility

of polycrystalline samples was measured between 4 and 300 K at field of 1 T using computer-controlled SQUID magnetometer. Diamagnetic correlations were made using Pascal's constants [15].

The pH of the solutions was monitored in a Digimed DMPH-2 instrument, coupled to a combined pH electrode, from Ingold or Radiometer. Appropriate buffer solutions were used to calibrate the instrument. Conductivity experiments with the complexes studied (in 1 mmol dm⁻³ aqueous solution) were carried out in a Digimed DM-31 instrument, using a 10.0 mmol dm⁻³ KCl solution as standard (specific conductivity = 1412.0 μS cm⁻¹, at 25 °C) [16].

2.4. Catalytic oxygenation studies

The catalyzed oxidation of 2,6-di-*tert*-butylphenol was performed under pseudo-first-order conditions, in a standard quartz cell with 10 mm optical length and 3.00 ml volume, at 25.0 ± 0.5 °C, in methanol solution following the formation of the corresponding diquinone or diphenoquinone, at 418 nm ($\epsilon = 5.48 \times 10^4 \text{ mol}^{-1} \text{ dm}^3 \text{ cm}^{-1}$). Kinetic experiments were carried out using [2, 6-di-*tert*-butylphenol] = 11.5 mmol dm⁻³ (2.0 ml), and [catalyst] = 0.090 mmol dm⁻³, except [Cu₄(apip)₄(im)₄]⁴⁺ = 0.045 mmol dm⁻³ (1.0 ml). Experimental curves of increasing absorbance as a function of time were analyzed by the initial rate method. Deviations in values of rate constants were ≤5% as indicated, estimated by repeated experiments. Analogous experiments for the oxidation of 3,4-dihydroxyphenylalanine (L-dopa) were carried out at 30.0 ± 0.5 °C, in aqueous solutions, monitoring the quinone formed at 475 nm ($\epsilon = 3.60 \times 10^3 \text{ mol}^{-1} \text{ dm}^3 \text{ cm}^{-1}$). For these experiments, the standard concentrations used were [L-dopa] = 6.67 mmol dm⁻³ and [catalyst] = 0.145 mmol dm⁻³, at pH 7.3 or 11.0.

3. Results and discussion

We have previously reported that some imidazole-bridged copper(II) complexes with tridentate imine ligands can act as good functional models of the tyrosinase enzyme [13]. Two new dinuclear copper(II) complexes in this series, species **1** and **2**, were now prepared and characterized by different

techniques. Other two similar complexes containing an imidazole group inserted in a tetradentate diimine ligand, and additionally phenolate bridges, species **3** and **4**, were also isolated. Schematic structures of the complexes are shown in Fig. 1. These species were obtained by condensation reaction of the carbonyl compounds, 2-acetylpyridine, salicylaldehyde, or 2-imidazolecarboxylaldehyde, with the amines 2-(2-aminoethyl)pyridine, 1,2-diaminoethane, 1,2-phenylenediamine, or *N*-benzyl-1,3-propanediamine, followed by metallation with copper(II) perchlorate, and finally by the addition of the imidazole, in the case of compounds **1** and **2**.

Elemental analysis results (≤0.6%) were consistent with the proposed formulae, corroborated by conductivity measurements, as shown in Section 2. The prepared complexes were additionally characterized by spectroscopic techniques (UV-Vis, IR, and EPR).

3.1. Electronic spectra

Electronic spectra of the copper complexes were carried out in aqueous solution, methanol, or DMF, and the corresponding data are given in Table 1. The broad band observed in the region 598–630 nm was assigned to the d–d transition [17], except to compounds **1** and **2**, where they are clouded. The shoulders or peaks observed at 311–430 nm were assigned to the imidazolate- or phenolate-copper charge transfer transition [18]. The intense band observed at 196–282 nm is mainly attributed to a $n \rightarrow \pi$, and a usually clouded $n \rightarrow \pi^*$ transitions in the ligands. For species **3** and **4**, the corresponding spectra exhibited analogous bands, as shown in Fig. 2. However, substantial shift of the bands in the visible range to higher wavelengths were verified, attributed to an increasing electronic density at species **4**, when compared to species **3**.

In aqueous solution, all these compounds bridged by imidazolate- or phenolate ligands showed an equilibrium with the corresponding mononuclear species, very dependent on the pH, similarly to that observed before [13]. In alkaline medium, the dinuclear species are predominant, and for two of the studied complexes, species **3** and **4** containing phenolate bridges, it was also observed a dependence of the corresponding equilibrium on the concentration of the complex. In Fig. 3, curves of absorbance versus

Table 1
Main bands in the UV-Vis spectra of the copper(II) complexes prepared

Compounds	λ_{\max} (nm) (ϵ , $10^3 \text{ M}^{-1} \text{ cm}^{-1}$)		λ_{\max} (nm) (ϵ , $\text{M}^{-1} \text{ cm}^{-1}$) d-d band
	$n \rightarrow \pi$, or $n \rightarrow \pi^*$ transitions	LCMT bands $\pi \rightarrow d\pi$	
$[\text{Cu}_2(\text{apph})_2\text{im}](\text{ClO}_4)_3$ (1) (this work)	268 (29.4)	334 (19.1); 430 (8.7) (sh)	–
$[\text{Cu}_2(\text{apbz})_2\text{im}](\text{ClO}_4)_3$ (2) (this work)	268 (22.7)	382 (5.9)	–
$[\text{Cu}_2(\text{iensal})_2](\text{ClO}_4)_2$ (3) (this work)	223 (44.9); 236 (42.7); 269 (29.2)	311 (12.9); 360 (9.8)	598 (428)
$[\text{Cu}_2(\text{iphalsal})_2](\text{ClO}_4)_2 \cdot \text{CH}_3\text{OH}$ (4) (this work)	208 (68.8); 241 (60.1)	322 (54.9); 383 (52.2)	596 (sh)
$[\text{SECu}(\text{im})\text{CuSE}]\text{ClO}_4$ (5) [13]	196 (28.9); 216 (31.3); 235 (33.5); 263 (17.0)	350 (6.6)	605 (133)
$[\text{Cu}_2(\text{apip})_2\text{im}](\text{ClO}_4)_3 \cdot \text{H}_2\text{O}$ (6) [13]	200 (59.6); 254 (17.5); 282 (15.5)	–	630 (137)
$[\text{Cu}_4(\text{apip})_4(\text{im})_4](\text{ClO}_4)_4 \cdot 2\text{H}_2\text{O}$ (7) [13]	200 (59.7); 254 (17.4); 282 (15.2)	–	624 (158)

^a Spectra in aqueous *N,N*-dimethylformamide.

^b Spectra in aqueous methanol solution.

wavelength, for the compound $[\text{Cu}_2(2\text{-iphalsal})_2]^{2+}$ **4** in the concentration range $5\text{--}20 \mu\text{mol dm}^{-3}$, showed significant differences in the relative intensities of bands at 310 and 322 nm. Further, a 10 nm-shift was observed in the band around 390 nm, assigned to the LMCT transition $\pi(\text{phenolate}) \rightarrow d\pi(\text{Cu(II)})$, with increasing concentrations of the complex. These spectral changes are indicative of the equilibrium shifting to the dinuclear species at higher concentrations.

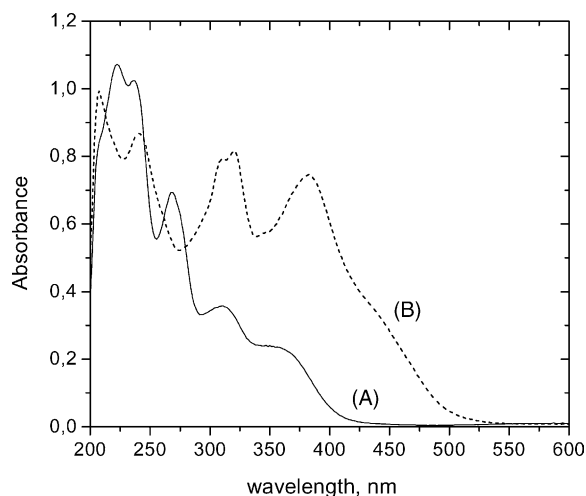


Fig. 2. Electronic spectra of the $[\text{Cu}_2(\text{iensal})_2]^{2+}$ **3** and $[\text{Cu}_2(\text{iphalsal})_2]^{2+}$ **4** complexes in methanol solution. (A) [Complex **3**] = $2.5 \times 10^{-5} \text{ mol dm}^{-3}$, and (B) [complex **4**] = $1.5 \times 10^{-5} \text{ mol dm}^{-3}$.

3.2. EPR spectra

With the aim of comparing the geometric environment around copper ions in those complexes, spectroscopic studies by EPR were then carried out. Spectra in frozen methanol/water (4:1, v/v) solutions, at 77 K, are shown in Fig. 4, illustrating both the signals at $g \sim 2$, around 3100 G, and also at $g \sim 4$, around 1500 G. As expected, the $g \sim 4$ signal, characteristic of a weak exchange interaction between

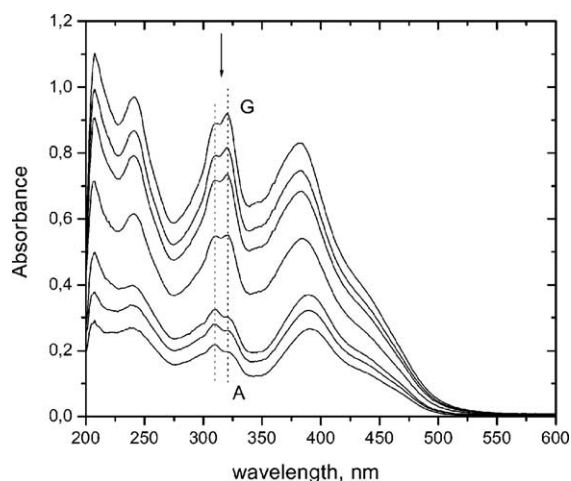


Fig. 3. Absorbance curves, in the range 200–600 nm, for the $[\text{Cu}_2(\text{iphalsal})_2]^{2+}$ **4** complex, in methanol solution. [Complex] ($\times 10^{-6} \text{ mol dm}^{-3}$) = (A) 5.00; (B) 7.50; (C) 8.75; (D) 10.0; (E) 12.5; (F) 15.0; (G) 20.0.

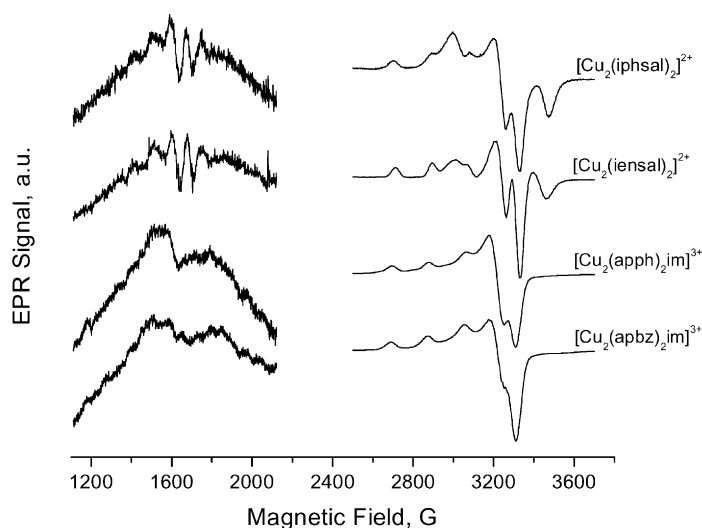


Fig. 4. EPR spectra of the copper(II) complexes studied (~ 3 mM), in frozen methanol/water (4:1, v/v) solutions, at $g \sim 2$ and 4 regions ($\sim 100\times$). **1**, gain = 5.64×10^3 , 3.17×10^5 ; **2**, gain = 4.48×10^3 , 3.17×10^5 ; **3**, gain = 4.48×10^3 , 3.17×10^5 ; **4**, gain = 3.17×10^3 , 8.93×10^6 .

the copper centers, is more pronounced in those species bounded by phenolate bridges. The corresponding parameters were determined, and shown in Table 2.

All the prepared complexes exhibited a tetragonal symmetry with the unpaired electron in the dx^2-y^2 orbital, as indicated by comparing the empirical ratio $g_{\parallel}/A_{\parallel}$, frequently used to evaluate tetrahedral distortions in tetragonal structures of copper(II) compounds [19]. Based on these data, a square-pyramidal coordination geometry is expected to the pentacoordinated complexes **3** and **4**. X-ray analysis for similar complexes has been recently published [20], corroborating that geometry.

3.3. IR spectroscopy

The registered IR spectra for these complexes, in KBr pellets, showed the expected characteristic bands of diimine compounds, as indicated in Section 2. Bands attributed to O–H and N–H bond stretching were observed around 3400 and 3200 cm^{-1} , respectively. Further, the stretching frequencies for C–H bonds in aliphatic CH, CH_2 , and CH_3 groups, or aromatic C–H bonds were observed around 3070 – 2921 cm^{-1} , while bands attributed to aliphatic or aromatic CH bending were verified in the 993 – 738 cm^{-1} range. The characteristic C=N bond stretching frequency was found at 1672 – 1600 cm^{-1} , followed

Table 2
EPR parameters of the copper(II) complexes studied

Compounds	EPR parameters ^a			
	g_{\parallel}	g_{\perp}	A_{\parallel} (10^{-4} cm^{-1})	$g_{\parallel}/A_{\parallel}$ (cm)
$[\text{Cu}_2(\text{apph})_2\text{im}](\text{ClO}_4)_3$ (1) (this work)	2.232	2.059	192	116
$[\text{Cu}_2(\text{apbz})_2\text{im}](\text{ClO}_4)_3$ (2) (this work)	2.242	2.058	195	115
$[\text{Cu}_2(\text{iensal})_2](\text{ClO}_4)_2$ (3) (this work)	2.229	2.053	189	118
$[\text{Cu}_2(\text{iphsal})_2](\text{ClO}_4)_2 \cdot \text{CH}_3\text{OH}$ (4) (this work)	2.228	2.056	196	114
$[\text{SECu}(\text{im})\text{CuSE}](\text{ClO}_4)$ (5) [13]	2.224	2.053	196	113
$[\text{Cu}_2(\text{apip})_2\text{im}](\text{ClO}_4)_3 \cdot \text{H}_2\text{O}$ (6) [13]	2.237	2.052	185	121
$[\text{Cu}_4(\text{apip})_4(\text{im})_4](\text{ClO}_4)_4 \cdot 2\text{H}_2\text{O}$ (7) [13]	2.239	2.054	185	121

^a In frozen methanol/water (4:1, v/v) solution, at 77 K.

by aromatic C=C stretching at 1565–1526 cm⁻¹. All the complexes prepared showed additionally bands at 1090 and 630 cm⁻¹, characteristic of non-coordinated perchlorate ions.

3.4. Magnetic properties

The solid-state dependence of magnetic data for complex **5** was reported previously [21]. Here, solid-state magnetic susceptibility measurements on polycrystalline samples of complexes **1–4** and **6** were made, in the temperature range 2–300 K.

The main magnetic interaction in those systems has a dimeric character that can be calculated within the framework of the Bleaney–Bowers equation [22]. The two ions interact through several intervening ligands in which the exchange interaction $H = -2JS_1S_2$ is given by the summation over the two atoms of the dinuclear molecule. In this isotropic Heisenberg Hamiltonian, a negative value of J refers to an anti-ferromagnetic interaction within the dimer, and positive J refers to ferromagnetic one. Usually a temperature-independent contribution to the susceptibility is also present. This includes the paramagnetic Van Vleck contribution, and the diamagnetic contribution of the ligands and anions. This is dealt with the introduction of a term $N\alpha$. The small temperature-dependent paramagnetic contribution of free monomers (with concentration $P \ll 1$), that may be present in the samples, has to be included in the final expression for the susceptibility:

$$\chi = \frac{2N\beta^2 g^2}{kT} \left[3 + \exp\left(\frac{-2J}{kT}\right) \right]^{-1} (1-p) + \left[\frac{N\beta^2 g^2}{2kT} \right]_p + N\alpha \quad (1)$$

Measurements of the magnetic susceptibility, $\chi = M/H$, were performed on powder samples in the temperature range 1.8–290 K, using a SQUID magnetometer. The magnetization M was measured in fields ranging from 100 to 2000 Oe. Above 1000 Oe, a slight dependence of M/H with the applied field was observed. Our results for the complexes **3** and **6** are plotted in Fig. 5. The results correspond to the data taken at 500 Oe, and are expressed in emu/mol of dimers. In this figure, the dashed lines are the result to the fit to the corrected Bleaney–Bowers Eq. (1). Table 3 summarizes the results of the fits to Eq. (1) for the new

dinuclear species **3**, **4** and **6**, compared to the previously studied complex **5** [21].

In order to complete the analysis of the samples, measurements with the mononuclear complex corresponding to species $[\text{Cu}_2(\text{apip})_2\text{im}]^{3+}$ **6**, that is the isolated compound $[\text{Cu}(\text{apip})\text{imH}](\text{ClO}_4)_2$, was also performed, and fitted to a Curie–Weiss law:

$$\chi = \frac{N\beta^2 g^2 S(S+1)}{[3k(T-\theta)]} + N\alpha \quad (2)$$

The parameters found for Eq. (2) were:

$$g = 2.0, \quad \theta = -0.21 \text{ K} \quad \text{and} \quad N\alpha = 0.000$$

The increase in χ at lower temperatures is due to a monomeric impurity. Note that the monomer concentration ρ is small in all cases, except for compounds **1** and **2** that exhibited a greater increase in susceptibility at the lowest temperature. This is probably due to a greater amount of the corresponding monomer as impurity. The value of the exchange constant for **6** ($2J/k = -65 \text{ cm}^{-1}$) is anti-ferromagnetic, and its value is of the same order of magnitude found in other similar system **5**, where the ligands that mediate the superexchange interaction are the same [21], in this case the imidazolate group. This is clear from Fig. 5B, where a distinctive maximum is present in the χ versus T curve, around 50 K. In contrast, in the compounds **3** and **4** where the interaction is mediated by a phenolate bridge, a small anti-ferromagnetic interaction is found, when the maximum in the curve occur around 2 K, as shown in Fig. 5A. This magnetic behavior for the different dinuclear copper(II) complexes may indicate the importance of the bonding angle in determining the sign of the Heisenberg coupling, generally used to find correlations between structure features and magnetic coupling in imidazolate- or phenolate-bridged copper(II) complexes [21,23].

3.5. Tyrosinase and catechol oxidase activity

The catalytic activity of these studied complexes in the oxidation of phenolic substrates was also verified. Kinetic experiments, using [2,6-di-*tert*-butylphenol] = 11.5 mmol dm⁻³, and [catalyst] = 0.090 mmol dm⁻³, except $[\text{Cu}_4(\text{apip})_4(\text{im})_4]^{4+}$ **7** = 0.045 mmol dm⁻³, were performed in methanolic solutions at 25.0 ± 0.3 °C, monitoring spectrophotometrically the corresponding diphenoquinone, at

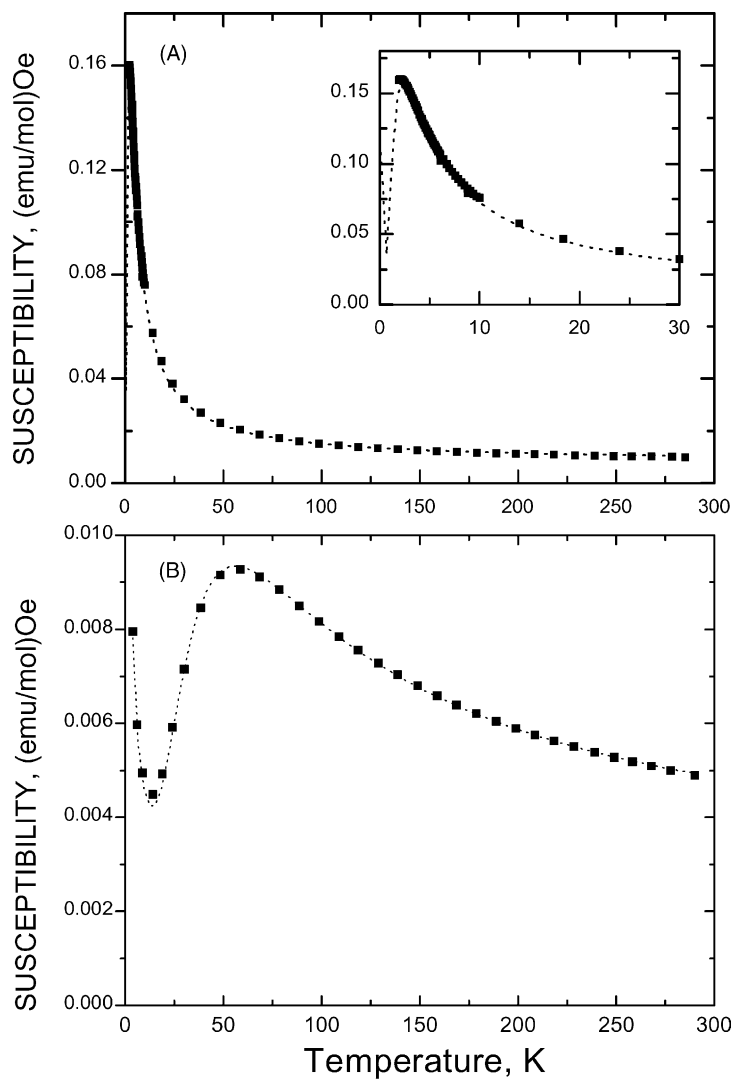


Fig. 5. Temperature dependence of the magnetic susceptibility, χ_M , for the compounds (A) **3**, and (B) **6**.

Table 3
Magnetic data for dinuclear imidazole- and phenolate-bridged copper(II) complexes

Compounds	$2J/k$ (cm^{-1})	g	ρ	$N\alpha$
$[\text{Cu}_2(\text{iensal})_2](\text{ClO}_4)_2$ (3)	-3.2	2.0	0.015	8×10^{-3}
$[\text{Cu}_2(\text{iphsal})_2](\text{ClO}_4)_2 \cdot \text{CH}_3\text{OH}$ (4)	-2.4	2.09	0.035	0.000
$[\text{SECu}(\text{im})\text{CuSE}](\text{ClO}_4)$ (5) ^a	-45	2.14	0	6×10^{-4}
$[\text{Cu}_2(\text{apip})_2\text{im}](\text{ClO}_4)_3 \cdot \text{H}_2\text{O}$ (6)	-65	2.0	0.03	2.5×10^{-3}

^a [21].

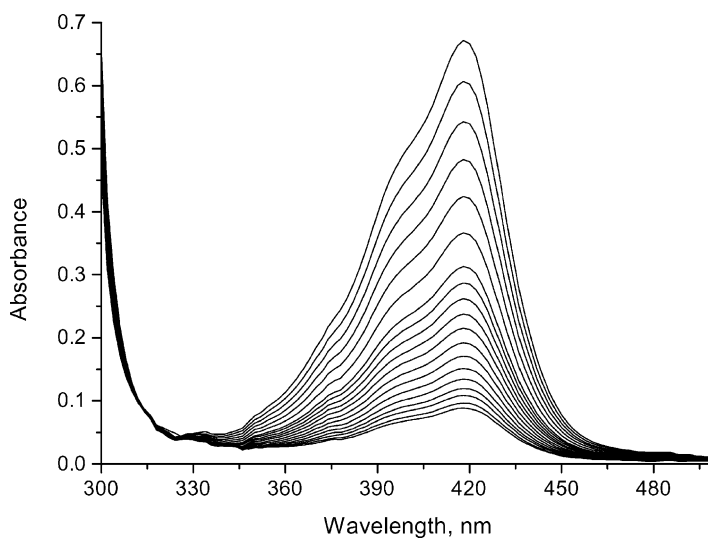


Fig. 6. Oxidation of 2,6-di-*tert*-butylphenol (11.5 mmol l^{-1}), at $25.0 \pm 0.5^\circ\text{C}$, in methanol solution, monitored at 418 nm. $[\text{Cu}_2(\text{apy-epy})_2\text{im}]^{3+} = 0.090 \text{ mmol dm}^{-3}$.

418 nm (Fig. 6). Some of the obtained results are illustrated in Fig. 7, showing that the most active catalysts were the tetranuclear $[\text{Cu}_4(\text{apip})_4(\text{im})_4]^{4+}$ **7**, and the dinuclear $[\text{Cu}_2(\text{appd})_2\text{im}]^{3+}$ **1** complexes, while the $[\text{Cu}_2(\text{iensal})_2]^{3+}$ **3**, $[\text{Cu}_2(\text{iphsal})_2]^{3+}$ **4**, and $[\text{SECu}(\text{im})\text{SECu}]^+$ **5** complexes were nearly inactive.

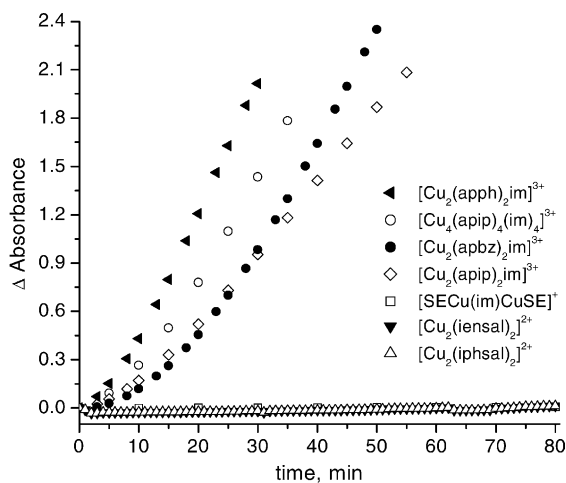


Fig. 7. Kinetic curves of the catalyzed oxidation of 2,6-di-*tert*-butylphenol ($11.5 \text{ mmol dm}^{-3}$) at $25.0 \pm 0.5^\circ\text{C}$, in methanol solution, monitored at 418 nm. [Catalyst] = $0.090 \text{ mmol dm}^{-3}$, except $[\text{Cu}_4(\text{apip})_4(\text{im})_4]^{4+} = 0.045 \text{ mmol dm}^{-3}$.

A steric match between the substrate and the copper centers, for the di- and tetranuclear complexes **1**, **2**, **6** and **7**, seems to be a determining factor in reactivity. The most active species was the complex $[\text{Cu}_2(\text{apph})_2\text{im}]^{3+}$ **1**, derived from phenylenediamine, and acetylpyridine, exhibiting a less distorted structure, in relation to the tetragonal one. For all the studied complexes, minimized structures were obtained using the HyperChem program version 5.1 (from Hypercube Inc., Gainsville, FL, USA), and the complex **1** showed the least steric hindrance between the ligands, allowing an easier coordination of the molecular dioxygen to the metal centers [24–26]. As in all the experiments, the quantity of copper ions were the same, the cavity dimension and/or its hydrophobic character are probably also important factors in determining the reactivity toward the used phenolic substrate, since the tetranuclear species **7** was more active than the corresponding dinuclear species [13].

The very low reactivity of the compounds **3**, **4** and **5** could be explained by the equilibrium with the corresponding mononuclear species, usually much less catalytically active [27], or through the lower stability of the complex when reduced. Complexes $[\text{Cu}_2(\text{iensal})_2]^{3+}$ **3**, and $[\text{Cu}_2(\text{iphsal})_2]^{3+}$ **4** are already pentacoordinated, and the complex $[\text{SECu}(\text{im})\text{CuSE}]^+$ **5**, exhibiting only one N_{imine} coordinated, is almost

Table 4

Kinetics parameters determined in the 2,6-di-*tert*-butylphenol oxidation catalyzed by diimine-copper(II) complexes

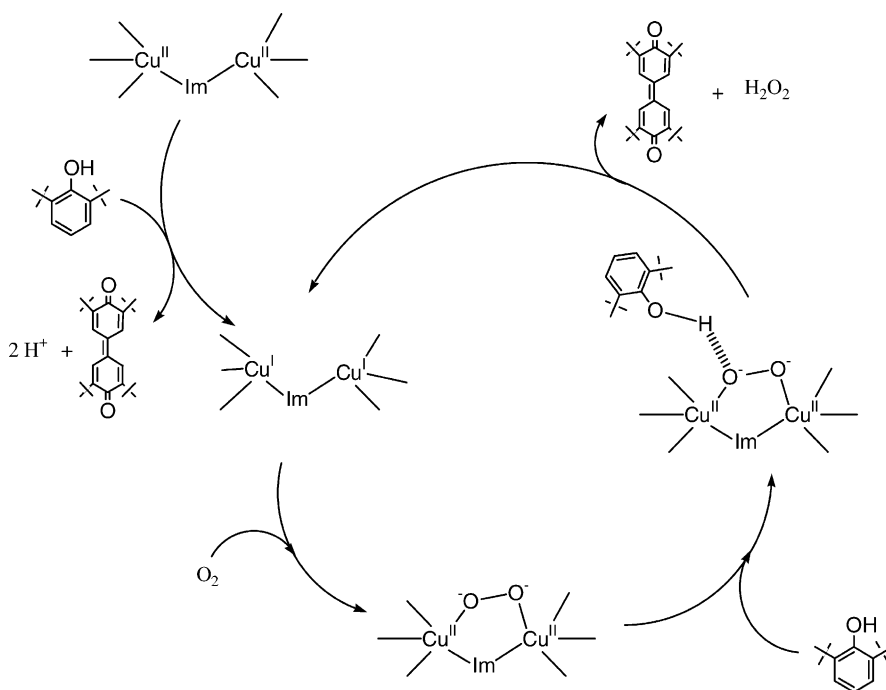
Compounds	k_3 (10^{-8} mol dm $^{-3}$ s $^{-1}$)	K_M (10^{-3} mol dm $^{-3}$)	k_{cat}/K_M (10^{-2} mol $^{-1}$ dm 3 s $^{-1}$)
[Cu ₂ (apph) ₂ im](ClO ₄) ₃ (1)	0.5	1.22	11.7
[Cu ₂ (apbz) ₂ im](ClO ₄) ₃ (2)	1.0	5.06	5.64
[Cu ₂ (apip) ₂ im](ClO ₄) ₃ ·H ₂ O (6)	0.3	1.41	6.73
[Cu ₄ (apip) ₄ (im) ₄](ClO ₄) ₄ ·2H ₂ O (7)	0.5	2.85	10.0

certainly decomposed after reduction of the metal centers, which could explain their inactivity.

The dependence of the reaction rate on the substrate concentration was also verified, by using increasing amounts of 2,6-di-*tert*-butylphenol, for the most active complexes **1**, **2**, **6** and **7**. A first-order dependence was observed at low concentrations of the substrate, whereas a saturation effect was found at higher concentrations. Those data fit to the Michaelis–Menten approach, and values for the k_3 and K_M kinetic parameters were obtained from the corresponding $1/V_i$ versus $1/[\text{phenol}]$ curves, shown on Table 4. In this approach, k_3 is the maximum velocity at saturating con-

centrations of the substrate, and K_M is the dissociation constant of the substrate from the catalyst–substrate complex [28].

The ratio k_{cat}/K_M is commonly used to compare the catalytic activity of different compounds. The values for the complexes **1** and **7** differ significantly from the other catalysts, showing that steric features on the ligands, and the presence of a hydrophobic cavity in the cyclic complex **7** are fundamental factors on determining the catalytic properties of these copper complexes. According to our results, and others in the literature for similar complexes acting as tyrosinase model [26,29], a catalytic cycle was proposed (Scheme 1), based on



Scheme 1.

the initial reduction of the metal centers by phenolic substrate, followed by the coordination of molecular oxygen to the copper ions. The phenolic substrate could interact directly with the coordinated dioxygen by hydrogen bonds, facilitating a $1e^-$ -transfer, and the concomitant formation of a phenoxyl intermediate, that would lead to the final product diphenoquinone, in a radical mechanism. Additional reactive oxygen species could be generated by the interaction of formed hydrogen peroxide with the copper centers. The non-enzymatic *o*-semi-quinone radical formation has been detected in vitro with native tyrosinase, by inverse disproportionation mechanism [30].

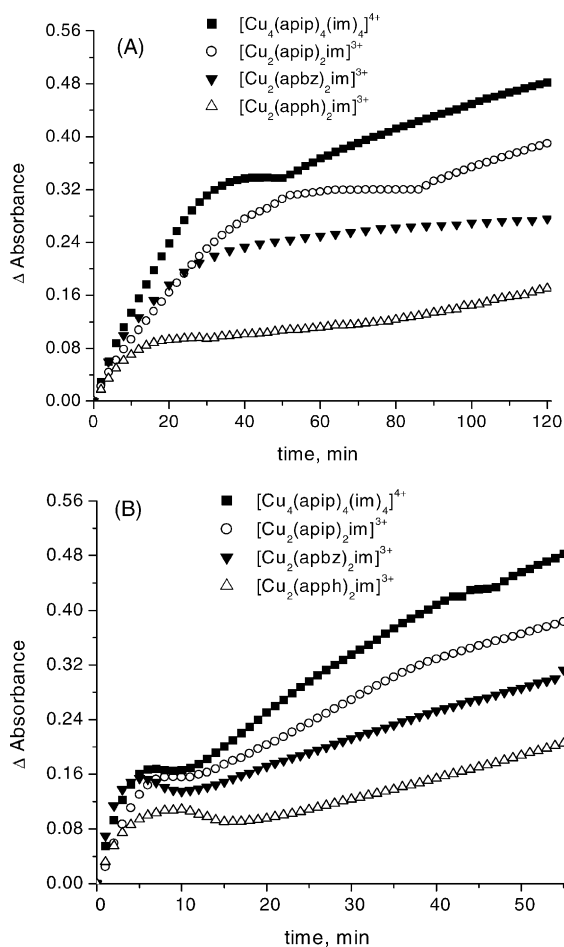


Fig. 8. L-dopa ($6.67 \text{ mmol dm}^{-3}$) oxidation, at $30.0 \pm 0.5^\circ\text{C}$, in phosphate buffer, monitored at 475 nm . [Catalyst] = $0.145 \text{ mmol dm}^{-3}$. (A) $\text{pH} = 7.30$; (B) $\text{pH} = 11.0$.

Similar studies, using L-dopa as the oxidizing substrate, indicated that the focused complexes are also good catalysts in the oxidation of catechols, leading to the corresponding quinone, and further to insoluble secondary products. The observed reaction rate increased with increasing pH, in the range 7–11 (as shown in Fig. 8), since higher pHs favor the dinuclear, or tetranuclear species. In this case, the tetranuclear compound **7** was also the best catalyst, followed by the correspondent dinuclear complex, $[\text{Cu}_2(\text{apip})_2\text{im}]^{3+}$ **6**. However, the complex $[\text{Cu}_2(\text{appd})_2\text{im}]^{3+}$ **1** showed lower activity than the others. This behavior could be explained by the polarity of the substrate, since L-dopa is more polar than 2,6-di-*tert*-butylphenol. The presence of extra pyridine rings on the species **6** and **7** could increase the polarity of these complexes, facilitating the interaction with the substrate L-dopa. Therefore, the hydrophobicity of the substrate seems to be other determining factor in the interaction with the metal complex.

4. Conclusions

On comparing the determined $2J$ values for the exchange anti-ferromagnetic interaction within the dinuclear species, a more pronounced interaction seems to ameliorate the catalytic activity. However, this is not a predominant effect, since the complex **5** is practically inactive. Additionally, for all the complexes studied those $2J$ values are much lower than that for the native enzyme ($-2J > 600 \text{ cm}^{-1}$). Also, the short Cu–Cu distance in compounds **3** and **4** do not provide best performance, probably because of a non-favorable bonding angle in the phenolate bridge.

Based on the determined kinetic parameters, very important factors on the reactivity of these compounds are the accessibility of the catalytic center, improved by hydrophobic (or hydrophilic) interactions between the substrates and the ligands. The more active catalysts were species **1**, **6** and **7**, that combine steric features with more accessible metal centers. Malachowski et al. [31] have reported similar effects on considering comparative catalytic studies for some other copper complexes. A steric match between the substrate and the copper centers is expected to be a determining factor in the process, since a significant difference between hemocyanin, an oxygen carrier, and tyrosinase

is thought to be the accessibility of the substrate to the active site [32].

However, the predominant factor on determining the catalytic activity of these studied complexes was the stability of the dinuclear (or tetranuclear) moiety in solution. Species more resistant to the equilibrium shift to the corresponding mononuclear species, with both the oxidation state of copper stabilized by a N₄-coordinating sphere (species **1**, **2**, **6** and **7**), were shown to be much more reactive towards both phenol and catechol substrates, in comparison to species surrounded by N₃O-coordinating ligands.

Acknowledgements

Financial support by the Brazilian agencies Fundação de Amparo à Pesquisa do Estado de São Paulo (FAPESP, Grants No. 99/05903-0, and 96/12051-1), and CNPq is gratefully acknowledged. W.A.A. also thanks FAPESP for fellowship (No. 98/15635-0) during his M.Sc. work. The authors would also like to thank Dr. J. Mattos for the use of the BOMEM 3.0 IR spectrometer.

References

- [1] (a) N. Kitajima, Y. Moro-oka, *Chem. Rev.* 94 (1994) 737; (b) W.B. Tolman, *Acc. Chem. Res.* 30 (1997) 227.
- [2] A. Sánchez-Ferrer, J.N. Rodríguez-López, F. García-Cánovas, F. García-Carmona, *Biochim. Biophys. Acta* 1247 (1995) 1.
- [3] J.A. Duine, J.A. Jongejan, in: J. Reedijk (Ed.), *Bioinorganic Catalysis*, Marcel Dekker, New York, 1993, Chapter 14, p. 447.
- [4] E.I. Solomon, D.W. Randall, T. Glaser, *Coord. Chem. Rev.* 200–202 (2000) 595.
- [5] S. Fox, K.D. Karlin, in: J.S. Valentine, C.S. Foote, A. Greenberg, J.F. Liebman (Eds.), *Active Oxygen in Biochemistry*, Blackie Academic and Professional, London, 1995, Chapter 4, p. 188.
- [6] A. Bakac, in: K.D. Karlin (Ed.), *Progr. Inorg. Chem.*, vol. 43, 1995, p. 267.
- [7] J.R.L. Walker, P.H. Ferrar, *Chemical Industry*, Gale Group, London, 1995, p. 836.
- [8] M.G. Peter, *Angew. Chem. Int. Ed. Engl.* 28 (1989) 555.
- [9] (a) C. Gendemann, C. Eicken, B. Krebs, *Acc. Chem. Res.* 35 (2002) 183; (b) C. Eicken, F. Zippel, K. Büldt-Karentzopoulos, B. Krebs, *FEBS Lett.* 436 (1998) 293.
- [10] P. Gentschev, N. Möller, B. Krebs, *Inorg. Chim. Acta* 300–302 (2000) 442.
- [11] M.F. Iskander, T.E. Khalil, R. Werner, W. Haase, I. Svoboda, H. Fuess, *Polyhedron* 19 (2000) 1181.
- [12] E. Monzani, G. Battaini, A. Perotti, L. Casella, M. Gullotti, L. Santagostini, G. Nardin, L. Randaccio, S. Geremia, P. Zanello, G. Opromolla, *Inorg. Chem.* 38 (1999) 5359.
- [13] W.A. Alves, I.A. Bagatin, A.M.D.C. Ferreira, *Inorg. Chim. Acta* 321 (2001) 11.
- [14] A. Puzari, J.B. Baruah, *J. Mol. Catal. A: Chem.* 187 (2002) 149.
- [15] R.L. Carlin, *Magnetochemistry*, Springer, Berlin, 1986.
- [16] W.J. Geary, *Coord. Chem. Rev.* 7 (1971) 81.
- [17] (a) B.J. Hathaway, D.E. Billing, *Coord. Chem. Rev.* 5 (1970) 143; (b) S. Keinan, D. Avnir, *J. Chem. Soc., Dalton Trans.* (2001) 941.
- [18] (a) E. Monzani, L. Quinti, A. Perotti, L. Casella, M. Gullotti, L. Randaccio, S. Geremia, G. Nardin, P. Faleschini, G. Tabbi, *Inorg. Chim. Acta* 37 (1998) 553; (b) C. Belle, C. Beguin, I. Gautier-Luneau, S. Hamman, C. Philouze, J.L. Pierre, F. Thomas, S. Torelli, *Inorg. Chim. Acta* 41 (2002) 479.
- [19] Y. Xie, W. Bu, A. Sun-Chi Chan, X. Xu, Q. Liu, Z. Zhang, J. Yu, Y. Fan, *Inorg. Chim. Acta* 310 (2000) 257.
- [20] C.-H. Kao, H.-H. Wei, Y.-H. Liu, G.-H. Lee, Y. Wang, C.-J. Lee, *J. Inorg. Biochem.* 84 (2001) 171.
- [21] J.-P. Costes, F. Dahan, M.B.F. Fernandez, M.I.F. Garcia, A.M.G. Deibe, J. Sanmartin, *Inorg. Chim. Acta* 274 (1998) 73.
- [22] B. Bleaney, K.D. Bowers, *Proc. R. Soc., London, Ser. A* 214 (1952) 4519.
- [23] Y.-H. Chung, H.-H. Wei, Y.-H. Liu, G.-H. Lee, Y. Wang, *J. Chem. Soc., Dalton Trans.* (1997) 1825.
- [24] M.R. Malachowski, B. Dorsey, J.G. Sackett, R.S. Kelly, A.L. Ferko, R.N. Hardin, *Inorg. Chim. Acta* 249 (1996) 85.
- [25] (a) E. Monzani, G. Battaini, A. Perotti, L. Casella, M. Gullotti, L. Santagostini, G. Nardin, L. Randaccio, S. Geremia, P. Zanello, G. Opromolla, *Inorg. Chim. Acta* 38 (1999) 5359; (b) E. Monzani, L. Casella, G. Zoppellaro, M. Gullotti, R. Pagliarin, R.P. Bonomo, G. Tabbi, G. Nardin, L. Randaccio, *Inorg. Chim. Acta* 282 (1998) 180.
- [26] A.E. Martell, R. Menif, P.M. Ngwenya, D.A. Rodkcliffe, *Bioinorganic Chemistry of Copper*, Chapman & Hall, New York, 1993, p. 325.
- [27] E. Spodine, J. Manzur, *Coord. Chem. Rev.* 119 (1992) 171.
- [28] D.B. Northrop, *J. Chem. Educ.* 75 (1998) 1153.
- [29] (a) C. Belle, C. Beguin, I. Gautier-Luneau, S. Hamman, C. Philouze, J.L. Pierre, F. Thomas, S. Torelli, E. Saint-Aman, M. Bonin, *Inorg. Chim. Acta* 41 (2002) 479; (b) D.A. Rockcliffe, A.E. Martell, *Inorg. Chim. Acta* 32 (1993) 3143.
- [30] R.P. Ferrari, E. Laurenti, E.M. Ghibaudi, L. Casella, *J. Inorg. Biochem.* 68 (1997) 61.
- [31] M.R. Malachowski, H.B. Huynh, L.J. Tomlinson, R.S. Kelly, J.W. Furbee jun, *J. Chem. Soc., Dalton Trans.* (1995) 31.
- [32] E.I. Solomon, U.M. Sundaram, T.E. Machonkin, *Chem. Rev.* 96 (1996) 2563.